

Actively Targeted Delivery of Doxorubicin to Bone Metastases by a pH-Sensitive Conjugation

WEI-LIANG YE,¹ YI-PU ZHAO,¹ REN NA,² FEI LI,¹ QI-BING MEI,³ MING-GAO ZHAO,³ SI-YUAN ZHOU¹¹Department of Pharmaceutics, School of Pharmacy, Fourth Military Medical University, Xi'an 710032, China²West Changle Sanatorium for Xi'an Army Retired Cadres of Fourth Military Medical University, Xi'an 710032, China³Department of Pharmacology, School of Pharmacy, Fourth Military Medical University, Xi'an 710032, China

Received 19 December 2014; revised 24 March 2015; accepted 16 April 2015

Published online 15 May 2015 in Wiley Online Library (wileyonlinelibrary.com). DOI 10.1002/jps.24476

ABSTRACT: Alendronate-monoethyl adipate-(hydrazone)-doxorubicin conjugate (ALN-MA-hyd-DOX) was synthesized to specifically deliver doxorubicin (DOX) to bone tumor tissue. The binding kinetics of ALN-MA-hyd-DOX with hydroxyapatite (HA) and natural bone were detected by using spectrophotometer. Cytotoxicity of ALN-MA-hyd-DOX on tumor cells was determined by MTT [3-(4,5-dimethylthiazol-2-yl)-2,5-diphenyl-tetrazolium bromide] method. The cellular uptake of ALN-MA-hyd-DOX was observed by using fluorescence microscopy. The *in vivo* antitumor activity of ALN-MA-hyd-DOX was investigated by using tumor-bearing nude mice model. The results indicated that ALN-MA-hyd-DOX was able to quickly bind with HA and natural bone. ALN-MA-hyd-DOX immobilized on the natural bone released more DOX in pH 5.0 medium than that in pH 6.0 or 7.4 medium. The cytotoxicity of ALN-MA-hyd-DOX toward A549 cells and MDA-MB-231/ADR cells was greater than DOX. ALN-MA-hyd-DOX was rapidly uptaken by A549 cells and MDA-MB-231/ADR cells. Compared with the same dose of free DOX, ALN-MA-hyd-DOX significantly decreased tumor volume of tumor-bearing nude mice. DOX mainly distributed in bone tumor tissue after ALN-MA-hyd-DOX was intravenously administered to tumor-bearing nude mice, whereas DOX distributed through the whole body after DOX was intravenously administered to tumor-bearing nude mice. These findings implied that the ALN-MA-hyd-DOX was a promising bone-targeted conjugate for treating bone neoplasms. © 2015 Wiley Periodicals, Inc. and the American Pharmacists Association *J Pharm Sci* 104:2293–2303, 2015

Keywords: bone-targeted drug delivery; doxorubicin; controlled release; alendronate; conjugation; p-glycoprotein; cytotoxicity; imaging methods; cancer

INTRODUCTION

Bone is a major organ for tumor metastasis, particularly for prostate and breast tumor. Although the tumor bone metastasis is not the major reason for causing death, symptoms associated with tumor bone metastasis such as bone pain, life-threatening hypercalcemia, nerve compression syndromes, and pathologic fractures significantly lowered the life quality of patients.^{1–3} Currently, there is a lack of effective treatments for patients with tumor bone metastasis. Therefore, it is imperative to develop effective methods to treat tumor bone metastasis.

It was reported that when tumor bone metastasis occurred, the acid-base balance in tumor bone metastasis tissue was broken, and osteoclasts secreted protons and acidic hydrolases into the bone resorption compartment, which led to the digestion of the mineral and organic phase of bone matrix.^{4,5} The pH value decreased to 4.5 in bone resorption microenvironment.⁶ Thus, a pH-sensitive bone-specific drug delivery system, the drug release of which is dependent on the environmental pH value, has attracted much attention.^{7,8} In our laboratory, hydrazone bond was used to prepare pH-sensitive site-specific drug delivery systems. The result showed that drug release was accelerated in acidic environment.^{9,10}

Bisphosphonates (BPs) are used to treat myeloma, osteoporosis, bone metastases, and other bone-related diseases in

the clinic.¹¹ Additionally, BPs can inhibit the angiogenesis of tumor tissue.^{12,13} BPs exhibit strong binding affinity with bone mineral.¹⁴ Therefore, BPs was used as excellent ligands for bone-targeted therapy.^{15,16} Alendronate (ALN), one of BPs, was approved by the US FDA (Food and Drug Administration) to treat osteoporosis, tumor-associated hypercalcemia, and several other bone-related diseases.^{17,18} Besides, ALN was proved to have antitumor effect in several tumor models.^{19–21} DOX has remained a widely used antitumor drug in the last decades, although it can cause serious systemic side effect, such as cardiotoxicity. In theory, if DOX is specifically delivered to the tumor bone metastases, its antitumor activity will be greatly enhanced and its systemic side effects will be significantly decreased.

In this paper, a new conjugate alendronate-monoethyl adipate-(hydrazone)-doxorubicin conjugate (ALN-MA-hyd-DOX) was synthesized to deliver DOX to the bone metastases by using monoethyl adipate (MA) as a linker. MA was conjugated with ALN and DOX by amide bond and hydrazone bond, respectively. The binding kinetics of ALN-MA-hyd-DOX with hydroxyapatite (HA) and natural bone was determined. The *in vitro* and *in vivo* antitumor activities of ALN-MA-hyd-DOX were investigated on the tumor-bearing nude mice model.

MATERIALS AND METHODS

Materials

Alendronate, HA, N-hydroxysuccinimide (NHS), and 1-ethyl-3-(3-dimethylaminopropyl) carbodiimide (EDCI) were purchased from J&K CHEMICA (Beijing, China). DOX was purchased

Correspondence to: Si-Yuan Zhou (Telephone: +86-29-84776783; Fax: +86-29-84776783; E-mail: zhousy@fmmu.edu.cn)

This article contains supplementary material available from the authors upon request or via the Internet at <http://wileylibrary.com>.

Wei-Liang Ye and Ren Na contributed equally to this work.

Journal of Pharmaceutical Sciences, Vol. 104, 2293–2303 (2015)

© 2015 Wiley Periodicals, Inc. and the American Pharmacists Association

from Hisun Pharmaceutical Company (Zhejiang, China). MA was purchased from Aladdin reagent Company (Shanghai, China). All other chemicals were of analytical grade and obtained from commercial suppliers without further purification. RPMI1640 medium, 4',6-diamidino-2-phenylindole, and 3-(4,5-dimethylthiazol-2-yl)-2,5-diphenyl-tetrazolium bromide (MTT) were bought from Invitrogen Technologies Company (Carlsbad, California). A549 cells were purchased from Institute of Biochemistry and Cell Biology, Chinese Academy of Science (Shanghai, China). MDA-MB-231/ADR cells were DOX-resistant human breast cancer cells, which were induced in our laboratory.

Methods

Synthesis of ALN-MA-hyd-DOX and ALN-MA-ami-DOX

The synthetic route of ALN-MA-hyd-DOX is shown schematically in Figure 1 according to the literature.²² MA (500 mg, 2.8 mmol) was dissolved in 10 mL ethanol, and then 4 mL hydrazine hydrate (6.9 mmol) solution was drop-wise added. The reaction mixture was refluxed for 12 h. Then the ethanol was removed from the reaction solution. The residue was extracted with diethyl ether for three times. The residue was spin-dried to get MA hydrazide. The product was purified by silica gel column.

Monoethyl adipate hydrazide (80 mg, 0.45 mmol) was dissolved in 10 mL methanol, and then DOX (140 mg, 0.25 mmol) and 60 μ L of trifluoroacetic acid were added. The reaction mixture was stirred for 12 h in the darkness at room temperature. After ethanol was removed from the reaction mixture, the MA-hyd-DOX was purified by silica gel column.

Monoethyl adipate-(hydrazine)-doxorubicin (230 mg, 0.33 mmol) was dissolved in 8 mL dimethyl sulfoxide (DMSO) and was activated by both 100 mg EDCI (0.515 mmol) and 80 mg NHS (0.695 mmol) for 12 h at room temperature. ALN (120 mg, 0.44 mmol) dissolved in 10 mL H₂O was drop-wise added to the reaction solution. Then, triethylamine was added to adjust pH of the reaction solution to 8–9. The reaction mixture was stirred for another 12 h at room temperature. Ethyl acetate was added to the reaction solution, and the resulting precipitate was filtered and rinsed three times with ethyl acetate, then purified by reversed-phase column chromatography. The yield was 173.6 mg (0.185 mmol, 49.4%). The purification of ALN-MA-hyd-DOX was analyzed according to previously reported method.¹⁰ Lipo-hydro partition coefficient (Log *P*) of DOX and ALN-MA-hyd-DOX was determined by using *n*-octanol/water method.¹⁰ The concentration of DOX (or ALN-MA-hyd-DOX) in both phases was measured by using Beckman DU-800 spectrophotometer.

The synthetic route of ALN-MA-ami-DOX is showed schematically in Figure 2. MA (80 mg, 0.45 mmol) was dissolved in 15 mL methanol, and then 104 mg NHS (0.91 mmol), 210 mg EDCI (1.08 mmol), and 70 μ L triethylamine were added. The reaction mixture was stirred at room temperature for 6 h, and then 160 mg DOX (0.29 mmol) was added. The reaction mixture was stirred for another 12 h. Finally, the ALN was conjugated with the MA-ami-DOX. The ALN-MA-ami-DOX was purified by reversed-phase column chromatography. The yield was 87.3 mg (0.094 mmol, 51.9%). The purification of ALN-MA-ami-DOX was analyzed according to a previously reported method.¹⁰ Log *P* of ALN-MA-ami-DOX was determined by using aforementioned method.

Binding Kinetics of DOX Conjugate with HA

The binding kinetics of ALN-MA-hyd-DOX, ALN-MA-ami-DOX, and DOX with HA were assessed according to the previous literature.^{23,24} Briefly, 1 mg conjugate was dissolved in 10 mL phosphate-buffered saline (PBS) in a falcon tube, and 100 mg HA was added. The mixture was gently shaken at 37°C in water bath. Another solution of conjugate without HA was used as control. After 0, 5, 10, 15, 20, 30, 40, 50, 60, 70, 80, and 90 min, the mixture solution was centrifuged (4000g, 5 min) and the absorbance of the supernatant was measured by Beckman DU-800 spectrophotometer at 233 nm. The binding percentage of conjugate with HA was calculated as by the formula: $[(OD_{\text{without HA}} - OD_{\text{with HA}})/(OD_{\text{without HA}})] \times 100\%$.

Binding Kinetics of DOX Conjugate with Natural Bone

Bone fragments, isolated from the backbone of pig, were cut into small pieces. The bone pieces were washed with water and ethanol and then dried in drying oven. One milligram DOX (or ALN-MA-ami-DOX, ALN-MA-hyd-DOX) was dissolved in 10 mL PBS in a falcon tube, after which 100 mg bone pieces were added. The mixture was gently shaken at 37°C in water bath. Another solution of conjugate without bone pieces was used as control group. After 0, 5, 10, 15, 20, 30, 40, 50, 60, 70, 80, and 90 min, the mixture solution was centrifuged (4000g, 5 min) and the absorbance of the supernatant was measured by Beckman DU-800 spectrophotometer at 233 nm. The binding percentage of conjugate with HA was calculated by the formula: $[(OD_{\text{without nature bone}} - OD_{\text{with nature bone}})/(OD_{\text{without nature bone}})] \times 100\%$.

DOX Release from DOX Conjugate at Different pH Medium

The mixture solution contained nature bone and ALN-MA-ami-DOX or ALN-MA-hyd-DOX was gently shaken in water bath at 37°C for 2 h. Then, it was centrifuged at 4000g for 5 min, and the supernatant was discarded. The precipitation was washed three times with 2.0 mL water. The precipitation was dispersed in 10 mL PBS (pH 5.0, 6.0, and 7.4) in falcon tube. The falcon tubes were then gently shaken in water bath at 37°C. After a predetermined time period, the mixture solution was centrifuged (4000g, 5 min) and the absorbance of the supernatant was measured by Beckman DU-800 spectrophotometer at 233 nm to calculate the amount of DOX released from the nature bone.

Cell Culture Condition

A549 cells, also called human lung cancer cell lines, are easy to metastasize to the bone.²⁵ A549 cells were maintained in a RPMI 1640 medium. MDA-MB-231/ADR cells, also called human DOX-resistant breast cancer cell line, are easy to metastasize to the bone.²⁶ MDA-MB-231/ADR cells were maintained in L-5 medium. All cell lines were supplemented with 100 units/mL penicillin, 100 units/mL streptomycin, 10% fetal bovine serum, and cultured in a humidified atmosphere containing 5% CO₂ at 37°C.

Cytotoxicity of DOX Conjugates

The A549 and MDA-MB-231/ADR cells were seeded in 96-well plates at a density of 1×10^4 cells per well and incubated for overnight to allow cells attachment. Then, cells were incubated

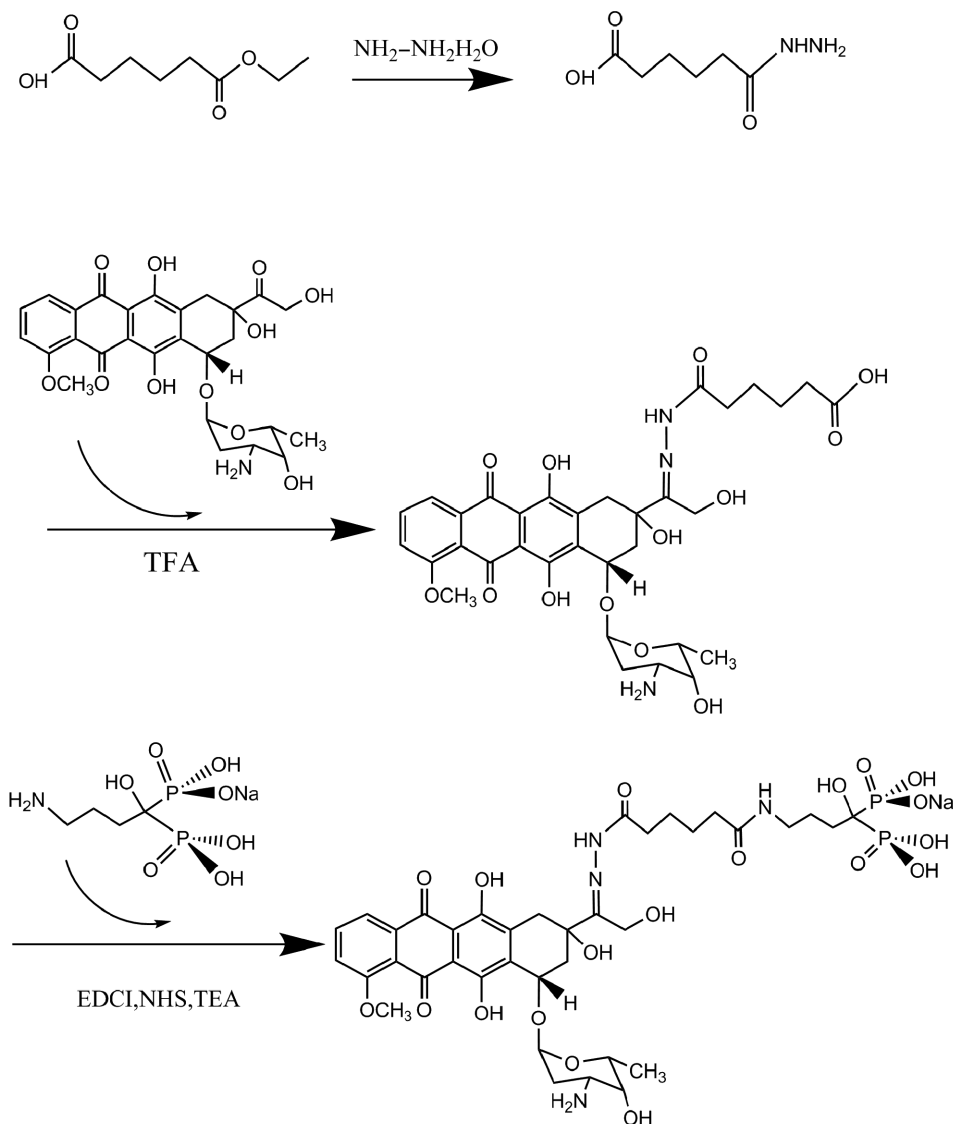


Figure 1. The synthetic route of ALN-MA-hyd-DOX.

with fresh medium containing various concentration of free DOX, ALN-MA-ami-DOX, or ALN-MA-hyd-DOX (0.08, 0.8, 8, and 40 $\mu\text{mol/L}$ DOX) for 24 or 48 h. MTT (5 mg/mL, 50 μL) was added and incubated for 4 h. After removing the medium, 150 μL of DMSO were added to dissolve formazan crystals. The absorbance was measured at 570 nm using a CODA Automated EIA Analyzer (Bio-Rad Laboratories, Hercules, California).

The Effect of DOX Conjugates on Cell Apoptosis

Apoptosis of tumor cells, induced by DOX conjugates, was observed by measuring the intracellular caspase-3 activities. The A549 cells or MDA-MB-231/ADR cells were treated with free DOX (ALN-MA-ami-DOX or ALN-MA-hyd-DOX) at the concentration of 10 $\mu\text{mol/L}$ DOX for 24 or 48 h. The cells were collected and lysed by lysate buffer. Then, the cells lysate were treated with 50 $\mu\text{mol/L}$ Ac-DEVD-AFC at room temperature for 60 min in darkness. The caspase-3 activity was determined by measuring the absorbance at 405 nm.

Cellular Uptake of DOX Conjugates

A549 cells and MDA-MB-231/ADR cells were seeded in cover-glass containing 24-well plates at a density of 1×10^5 cells per well and incubated for 24 h at 37°C. Then, free DOX (ALN-MA-ami-DOX or ALN-MA-hyd-DOX, 10 $\mu\text{mol/L}$) was added and incubated for 4 h at 37°C. The cells were washed three times with PBS and treated with 4',6-diamidino-2-phenylindole (10 $\mu\text{g/mL}$) for 15 min for nucleus staining. Then, the cells were washed with PBS for three times and fixed with 1.5% formaldehyde. Cover slips were placed onto microscope slides, and DOX uptake was observed by using 80i fluorescence microscope (Nikon Corporation, Tokyo, Japan).

Antitumor Activity of ALN-MA-hyd-DOX In Vivo

Female athymic nude mice (body weight = 20–23 g) were injected via intratibia with A549 cells (1×10^7 cells/animal). There were four mice in each group. Treatment was initiated on the 10th day after tumor cell inoculation. Normal saline, free DOX (10 $\mu\text{mol/kg}$) and ALN-MA-hyd-DOX (10 $\mu\text{mol/kg}$),

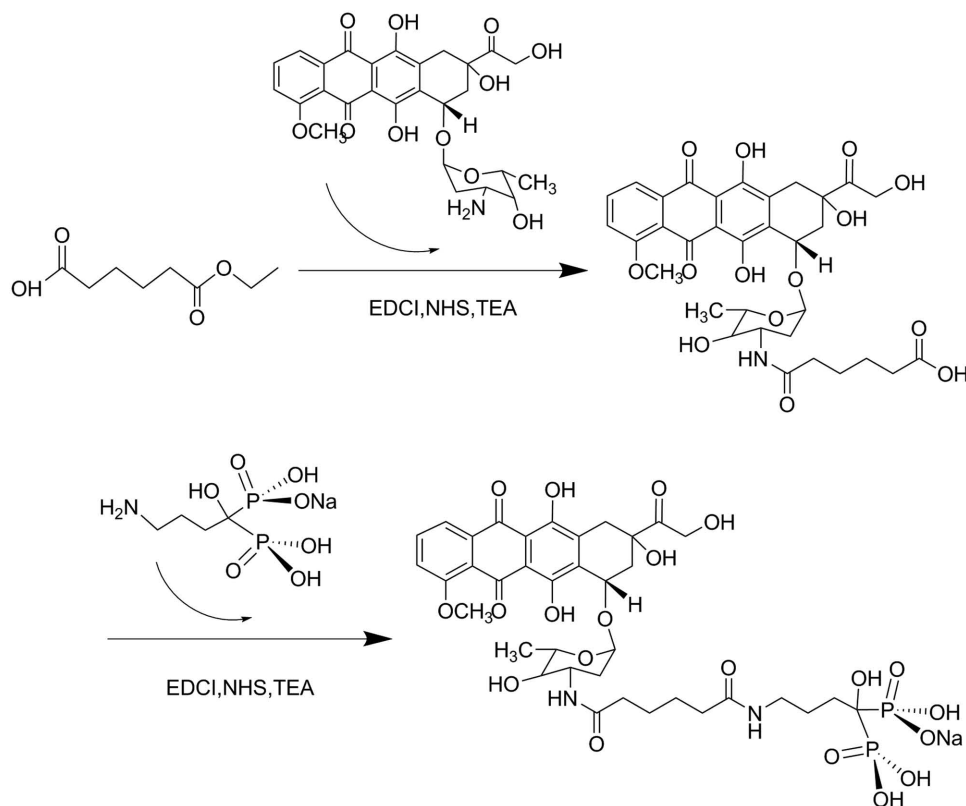


Figure 2. The synthetic route of ALN-MA-ami-DOX.

was injected to tumor-bearing nude mice via the tail vein for every 7th day (day 1, 7, and 14). Mice were observed every 3 days. The body weight was recorded and the tumor growth was monitored by using caliper. The tumor volume was calculated by using the formula: $\text{volume} = LW^2/2$ (L is the long diameter and W is the short diameter of a tumor). DOX usually leads to the damage of heart and kidney. Thus, at the end of the treatment, the heart and kidney samples were removed and stained by hematoxylin and eosin (H&E) to observe tissue injury.

Biodistribution Study

Female athymic nude mice (body weight = 20–23 g) were injected intratibia with A549 cells (1×10^7 cells/animal). When the tumor volume reached about 300 mm^3 , free DOX ($10 \mu\text{mol/kg}$) and ALN-MA-hyd-DOX ($10 \mu\text{mol/kg}$) were administered to tumor-bearing nude mice by tail vein injection. Twelve hours after the injection, major organs including heart, liver, spleen, kidney, lung, and bone in tumor tissue were removed. The fluorescence intensity in organs and bone tumor tissues was observed and semiquantitative by the Caliper IVIS Lumina *in vivo* image (Caliper Life Science, Boston, MA, USA).

Statistical Methods

Experiments were performed in triplicates. The results are expressed as mean \pm SD. Statistical analyses were performed with Graph Pad Prism 5.0.

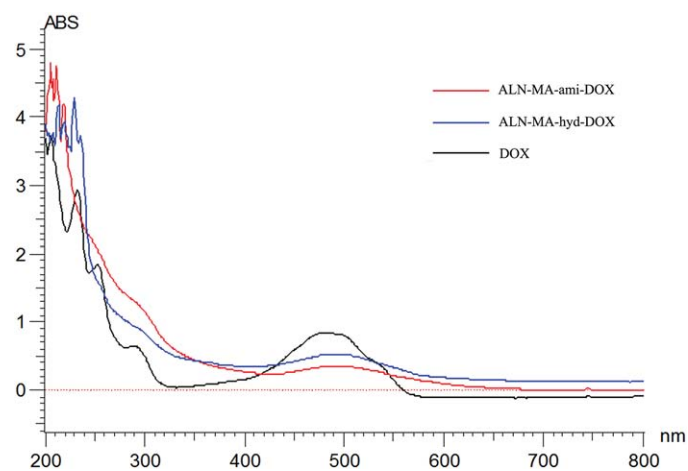


Figure 3. The ultraviolet spectrum of DOX, ALN-MA-ami-DOX, and ALN-MA-hyd-DOX.

RESULTS

Characterization of ALN-MA-hyd-DOX and ALN-MA-ami-DOX

The typical HPLC chromatogram of ALN-MA-hyd-DOX is shown in Supplementary Figure 1a. The purity of ALN-MA-hyd-DOX was 98.7%. The ultraviolet spectrum of ALN-MA-hyd-DOX is shown in Figure 3. The results indicated that there were significant difference in ultraviolet spectrum between DOX and ALN-MA-hyd-DOX. The mass spectrum, IR spectrum, and ^1H NMR spectrum of ALN-MA-hyd-DOX are shown in Supplementary Figures 1b–1d, respectively. The molecular ion peak

Table 1. Molecular Properties of DOX Conjugates ($n = 5$)

Compound	Log P	Molecular Weight	Number of Oxygen and Nitrogen Atoms	Number of –OH and –NH	Violations of Rule of Five	Number of Rotatable Bonds
DOX	0.33 ± 0.08	543	12	6	3	5
ALN-MA-ami-DOX	–0.163 ± 0.04	924	22	11	3	12
ALN-MA-hyd-DOX	–0.424 ± 0.11	938	23	12	3	12

($[M+H]^+$) of ALN-MA-hyd-DOX was 938. In IR spectrum of ALN-MA-hyd-DOX, peak at 3300–3500 was because of amino bond stretching bands; peak at 1634 was because of the C=C stretching vibration band; peak at 1608 was because of the hydrazone bond stretching vibration band; peaks at 451 and 540 were because of the O-P-O stretching bands; peak at 1362 was because of the P=O vibration band.^{27,28} The ^1H NMR spectrum of ALN-MA-hyd-DOX confirmed the presence of the MA moiety (signal at 1.2, 2.5, and 3.4 ppm) and the ALN moiety (signal at 4.6, 3.9, 3.6, 3.4, and 2.9 ppm). Conjugation of DOX was confirmed by the presence of signal at 8.0, 7.8, 7.5, 5.4, 2.1, and 1.9 ppm.

The typical HPLC chromatogram of ALN-MA-ami-DOX is shown in Supplementary Figure 2a. The purity of ALN-MA-ami-DOX was 97.9%. The ultraviolet spectrum of ALN-MA-hyd-DOX is shown in Figure 3. The mass spectrum, IR spectrum, and ^1H NMR spectrum of ALN-MA-ami-DOX are respectively shown in Supplementary Figure 2b–2d. The molecular ion peak ($[M+H]^+$) of ALN-MA-ami-DOX was 924. In IR spectrum of ALN-MA-ami-DOX, peak at 3300–3500 was because of amino bond stretching bands; peak at 1634 was because of the C=C stretching vibration band; peaks at 456 and 553 were because of the O-P-O stretching bands; peak at 1377 was because of the P=O vibration band.^{27,28} The ^1H NMR spectrum of ALN-MA-ami-DOX confirmed the presence of the MA moiety (signal at 1.3, 2.5, and 3.5 ppm) and the ALN moiety (signal at 4.2, 3.5, 3.4, and 2.6 ppm). Conjugation of DOX was confirmed by the presence of signal at 7.9, 7.6, 7.1, 5.2, 2.1, and 1.8 ppm.

Rule of five is a rule of thumb to evaluate whether a chemical compound with a certain pharmacological activity has properties to be an orally active drug in humans. Table 1 showed the molecular description of DOX, ALN-MA-ami-DOX, and ALN-MA-hyd-DOX, and there were three parameters that violated rule of five in DOX conjugates. Compared with free DOX, the water solubility of ALN-MA-ami-DOX and ALN-MA-hyd-DOX increased. This was an expected result caused by the substituent of ALN. There was no significant difference in water solubility between ALN-MA-ami-DOX and ALN-MA-hyd-DOX.

HA-Binding Kinetics of DOX Conjugates

The binding kinetics of DOX conjugates with HA is shown in Figure 4. Only a little amount of free DOX bounded with HA (<10%) in 90 min. However, ALN-MA-ami-DOX and ALN-MA-hyd-DOX bounded with HA very fast. About 62% of ALN-MA-ami-DOX and ALN-MA-hyd-DOX in the solution was bounded with HA in 20 min.

Binding Kinetics of DOX Conjugate with Natural Bone

As shown in Figure 5a, when free DOX was incubated with nature bone matrices at pH 7.4, only a little amount of DOX was bound with natural bone. In contrast, approximately 84% of ALN-MA-hyd-DOX was bounded with bone matrices in 30 min. The binding characteristics of ALN-MA-ami-DOX to

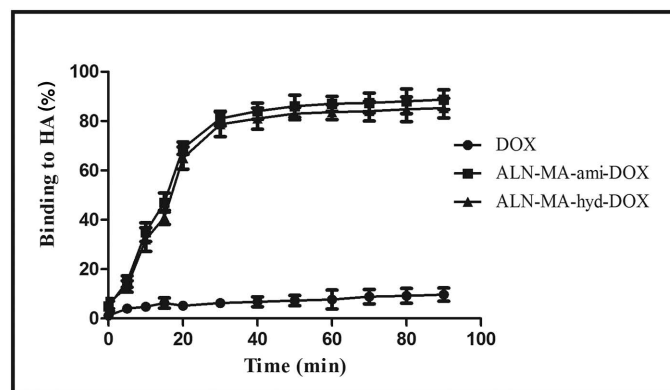


Figure 4. Binding kinetics of 1 mg DOX, ALN-MA-ami-DOX, and ALN-MA-hyd-DOX with the 100-mg bone mineral HA in 10 mL PBS. Data are presented as the average ± standard deviation ($n = 3$).

the nature bone matrices were similar to those of ALN-MA-hyd-DOX.

DOX Release from Natural Bone Matrices at Different pH Medium

The release of DOX from natural bone matrices that immobilized ALN-MA-hyd-DOX and ALN-MA-ami-DOX was investigated at different pH medium. As shown in Figure 5b, the release rate of DOX from immobilized ALN-MA-hyd-DOX was closely related to the medium pH. Natural bone matrices that immobilized ALN-MA-hyd-DOX released 73%, 43%, and 14% of the immobilized DOX at pH 5.0, 6.0, and 7.4 in 28 h, respectively. However, the rate that DOX released from immobilized ALN-MA-ami-DOX was independent on the medium pH. As shown in Figure 5c, after 28-h incubation, only 5% DOX was released from immobilized ALN-MA-ami-DOX in pH 7.4 medium, and 11% DOX was released in pH 5.0 medium. The above results implied that ALN-MA-hyd-DOX bound quickly with bone tissue and released DOX sustainedly at the bone tumor site.

Cytotoxicity of DOX Conjugate

As shown in Figure 6a, the viability of A549 cells in the ALN-MA-hyd-DOX-treated group was lower than that in ALN-MA-ami-DOX-treated group in 24 h. There was no significant difference in cytotoxicity between free DOX and ALN-MA-hyd-DOX on A549 cells in 24 h. However, as shown in Figure 6b, when the A549 cells were treated with ALN-MA-hyd-DOX for 48 h, the cell viability significant decreased, compared with the same dose of free DOX. The effects of free DOX, ALN-MA-ami-DOX, and ALN-MA-hyd-DOX on viability of MDA-MB-231/ADR cells are shown in Figure 7. ALN-MA-hyd-DOX showed greater cytotoxicity than free DOX in 24 or 48 h on MDA-MB-231/ADR cells. Compared with ALN-MA-ami-DOX, ALN-MA-hyd-DOX exhibited higher cytotoxicity on MDA-MB-231/ADR cells.

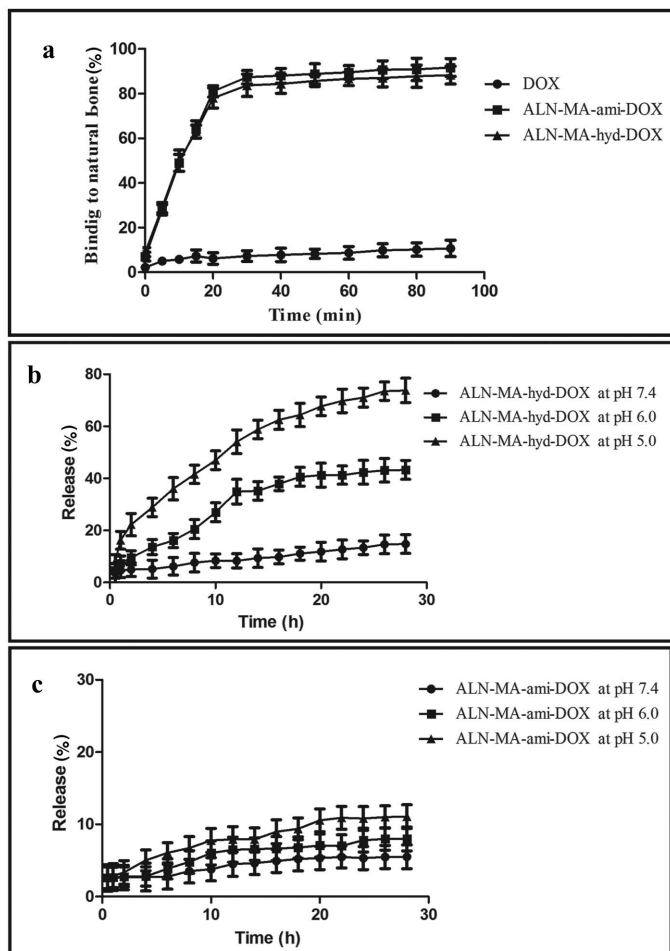


Figure 5. Binding kinetics of 1 mg DOX, ALN-MA-ami-DOX, and ALN-MA-hyd-DOX to 100 mg natural bone (a) in 10 mL PBS. The accumulative release of DOX from natural bone immobilized with ALN-MA-hyd-DOX (b) and ALN-MA-ami-DOX (c) at pH 5.0, 6.0, or 7.4. Data are presented as the average \pm standard deviation ($n = 3$).

Apoptosis Induced by DOX Conjugates

The cell apoptosis, induced by free DOX, ALN-MA-ami-DOX, and ALN-MA-hyd-DOX, was evaluated by measuring caspase-3 activity of the cells. When the cells were treated with ALN-MA-hyd-DOX for 24 h, as shown in Figure 8a, the caspase-3 activity in A549 cells and MDA-MB-231/ADR cells markedly increased. When the cells were treated with free DOX for 24 h, the level of caspase-3 in A549 cells significantly increased, but the level of caspase-3 activity in MDA-MB-231/ADR cells remained unchanged. When the cells were treated with ALN-MA-hyd-DOX for 48 h, as shown in Figure 7b, the level of caspase-3 in A549 cells and MDA-MB-231/ADR cells significantly increased, compared with 24 h treatment group. ALN-MA-ami-DOX did not significantly increase the level of caspase-3 in A549 and MDA-MB-231/ADR cells after 24 or 48 h treatment. These results were well consistent with the cytotoxicity of ALN-MA-ami-DOX and ALN-MA-hyd-DOX on A549 and MDA-MB-231/ADR cells.

Cellular uptake of DOX Conjugates

As DOX is fluorescent, cellular uptake of free DOX, ALN-MA-ami-DOX, and ALN-MA-hyd-DOX can be visualized by fluores-

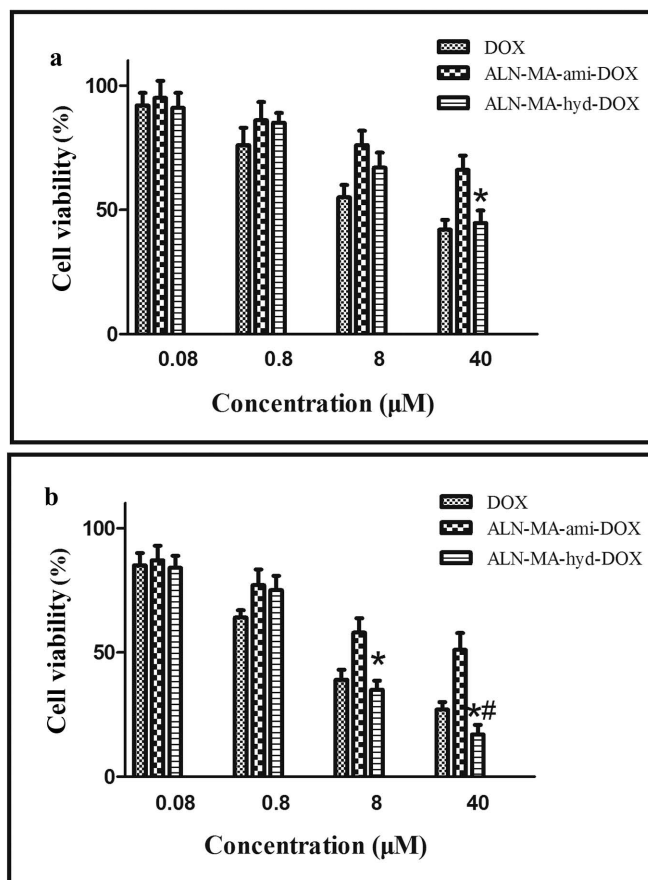


Figure 6. Cytotoxicity of DOX, ALN-MA-ami-DOX, and ALN-MA-hyd-DOX on A549 cells for 24 h (a) and 48 h (b) incubation. Data are presented as the average \pm standard deviation ($n = 5$). * $p < 0.05$ versus the same dose of ALN-MA-ami-DOX. # $p < 0.05$ versus the same dose of DOX ($n = 3$).

cence microscopy. As shown in Figure 9, the fluorescence was observed mainly in nucleus but little in cytoplasm when the A549 cells were incubated with free DOX for 4 h (Fig. 9a). However, as shown in Figure 9b, the red fluorescence was observed mainly in the cytoplasm and little in the nucleus when A549 cells were incubated with ALN-MA-ami-DOX for 4 h. When the A549 cells were incubated with ALN-MA-hyd-DOX for 4 h, as shown in Figure 9c, a similar pattern of cellular distribution with free DOX was observed. Little DOX was accumulated in the cytoplasm and nucleus (Fig. 10a) when MDA-MB-231/ADR cells were incubated with free DOX. The result was consistent with MTT result from the MDA-MB-231/ADR cells. When MDA-MB-231/ADR cells were treated with ALN-MA-ami-DOX, the fluorescence was observed in cytoplasm and nucleus (Fig. 10b). Stronger fluorescence was observed in nucleus when cells were incubated with ALN-MA-hyd-DOX for 4 h (10°C). The result indicated that ALN-MA-hyd-DOX could efficiently be uptaken by tumor cells and released DOX in tumor cells.

In Vivo Antitumor Activity of ALN-MA-hyd-DOX

The experiment results indicated that ALN-MA-hyd-DOX showed higher *in vitro* antitumor activity than ALN-MA-ami-DOX did. So, ALN-MA-hyd-DOX was chosen to evaluate its

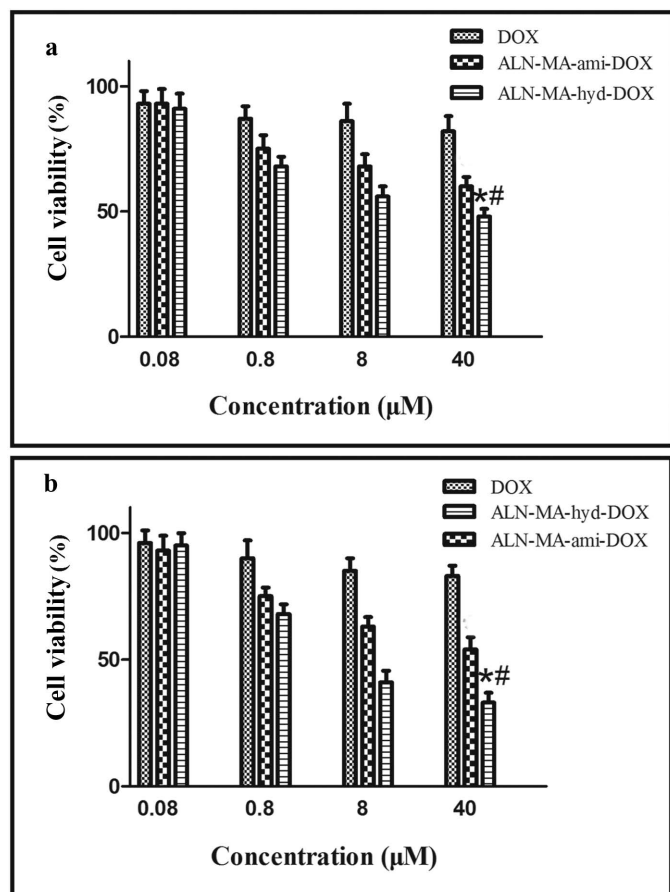


Figure 7. Cytotoxicity of DOX, ALN-MA-ami-DOX, and ALN-MA-hyd-DOX on MDA-MB-231/ADR cells for 24 h (a) and 48 h (b) incubation. Data are presented as the average \pm standard deviation ($n = 5$). * $p < 0.05$ versus the same dose of ALN-MA-ami-DOX. # $p < 0.05$ versus the same dose of DOX ($n = 3$).

in vivo antitumor activity by using free DOX as a control. The *in vivo* antitumor activity of the DOX and ALN-MA-hyd-DOX are shown in Figure 11. Figure 11a shows tumor growth after tumor-bearing mice were treated with normal saline, free DOX, and ALN-MA-hyd-DOX. The tumor volume in normal saline-treated mice increased very fast; ALN-MA-hyd-DOX significantly slowed tumor growth, compared with free DOX. Figure 11b shows body weight changes after tumor-bearing mice were treated with normal saline, free DOX, and ALN-MA-hyd-DOX. The decrease of body weight in free DOX-treated mice was 28.6% of original weight, which indicated the severe systemic side effects of DOX. In contrast, the body weight loss in ALN-MA-hyd-DOX-treated group was 9.5% of the original weight. This implied that the systemic side effects of ALN-MA-hyd-DOX were lower than those of free DOX. Figure 11c showed that ALN-MA-hyd-DOX significantly prolonged the survival time of tumor-bearing mice, compared with the free DOX. From Figure 11d, it can be clearly seen that ALN-MA-hyd-DOX significantly delayed the tumor growth, compared with the control mouse or free DOX-treated mouse.

In Vivo Targeting Ability of ALN-MA-hyd-DOX in Tumor-Bearing Mice

The biodistribution of DOX in tumor-bearing mice is shown in Figure 12a. After free DOX was intravenously adminis-

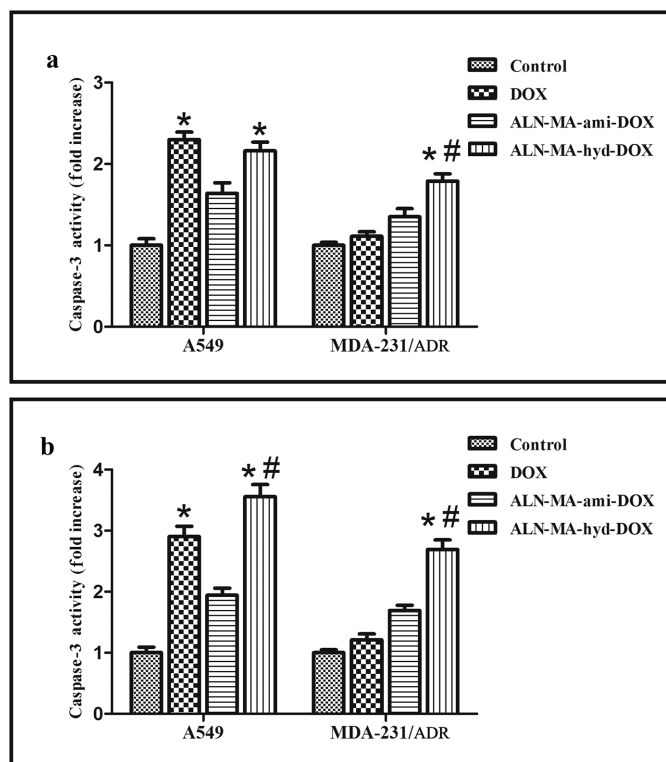


Figure 8. The effect of ALN-MA-ami-DOX and ALN-MA-hyd-DOX on caspase-3 activity in A549 cells and MDA-MB-231/ADR cells after 24 h (a) and 48 h (b) treatment. Data are presented as the average \pm standard deviation. * $p < 0.05$ versus control. # $p < 0.05$ versus DOX ($n = 3$).

tered to tumor-bearing mice, DOX accumulated in leg bone tumor tissue, heart, and kidney. However, after ALN-MA-hyd-DOX was intravenously administered to tumor-bearing mice, ALN-MA-hyd-DOX was mainly distributed in leg bone tumor

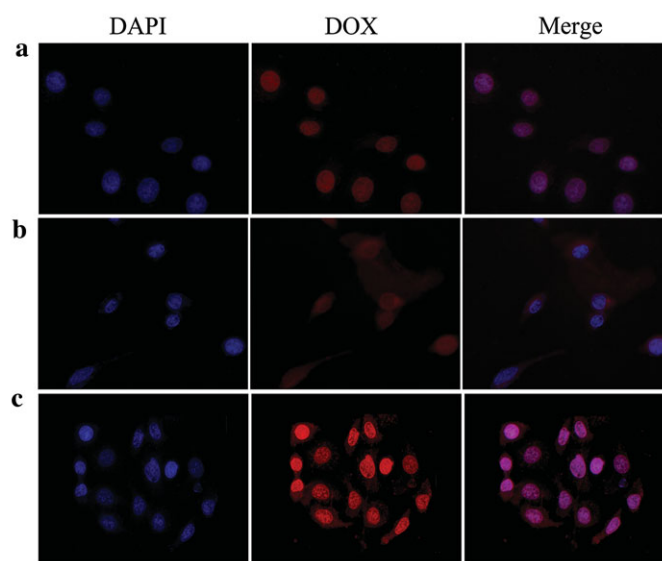


Figure 9. Intracellular localization of DOX (a), ALN-MA-ami-DOX (b), and ALN-MA-hyd-DOX (c) in A549 cells at an equivalent DOX concentration of 10 $\mu\text{mol/L}$ for 4 h incubation at 37°C. The pink region shows the localization of DOX (red) in the nucleus (blue).

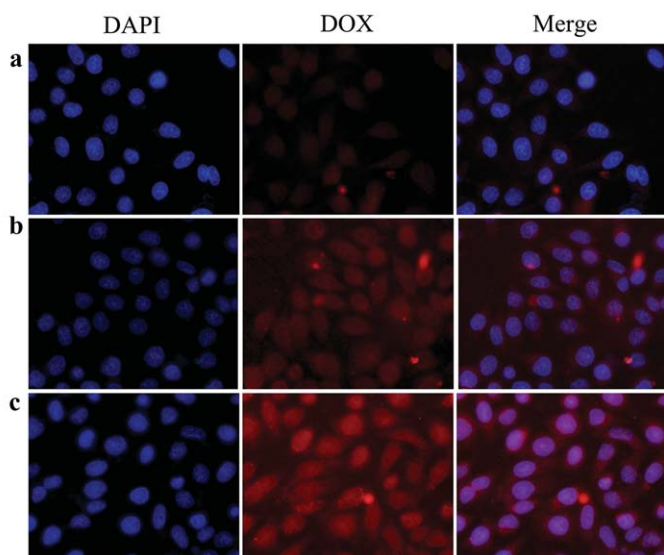


Figure 10. Intracellular localization of DOX (a), ALN-MA-ami-DOX (b), and ALN-MA-hyd-DOX (c) in MDA-MB-231/ADR cells at an equivalent DOX concentration of 10 $\mu\text{mol/L}$ for 4 h incubation at 37°C. The pink region shows the localization of DOX (red) in the nucleus (blue).

tissue, and a relatively lower amount of DOX was distributed in heart and kidney, compared with free DOX. The biodistribution of DOX was further semiquantitatively analyzed. The results are shown in Figure 12b. Compared with free DOX treatment, the fluorescence intensity in leg bone tumor tissue was significantly greater and the fluorescence intensity in heart and kidney was obviously lower after ALN-MA-hyd-DOX was intravenously administered to tumor-bearing mice. After ALN-MA-hyd-DOX was intravenously administered to tumor-bearing mice, the strongest fluorescence intensity was found in leg bone tumor tissue; the fluorescence intensity decreased in following order: liver, kidney, lung, heart, and spleen.

The Toxicity of ALN-MA-hyd-DOX in Heart and Kidney

The representative H&E staining sections of heart and kidney of tumor-bearing nude mice with different treatments are shown in Figure 13. Hearts from DOX-treated nude mice showed characteristic cardiotoxic lesions, including mild to moderate multifocal cardiomyocyte degeneration, vacuolation, interstitial edema, and mild inflammatory cell infiltrates. Hearts section from ALN-MA-hyd-DOX-treated mice appeared similar to those of normal saline-treated tumor-bearing mice. Compared with nude mice treated with normal saline, mice treated with free DOX caused significant kidney tubules pathological changes, including hyaline cast of kidney tubules. When tumor-bearing nude mice were treated with ALN-MA-hyd-DOX, the nephrotoxicity decreased as compared with the same dose of free DOX. These results indicated that ALN-MA-hyd-DOX treatment induced less cardiac and renal toxicity than free DOX.

DISCUSSION

Bone is one of the most common sites of metastasis in several epithelial tumors, such as breast tumor and prostate tumor.²⁸ However, treatment of bone metastatic tumor by radiation or

surgery is difficult because of the multiple metastatic sites and inaccessibility to the metastatic nodules.²⁹ Chemotherapy, the only currently available method to treat bone metastatic tumor, is limited by severe side effects to normal tissue.³⁰

The bone microenvironment is composed of osteoblasts, osteoclasts, mineralized bone matrix, and many other kinds of cells. Bone microenvironment is highly favorable for tumor invasion and growth. Tumor cells that metastasize to bone usually adhere to the endosteal surface. Cross-talk between bone microenvironment and tumor cells enhances a vicious cycle of tumor growth and bone destruction.^{31,32} Some factors that are secreted by tumor cells can stimulate osteoclast-mediated bone destruction and the consequent release of numerous factors immobilized within the bony matrix, which can act on tumor cells, promote more aggressive tumor metastasis and bone destruction. Tumor metastasis leads to the acidosis within bones.³³ The pH value can decrease to 4.5 in bone resorptive microenvironment.⁶ Recent studies have shown that the hydrazone bond between drug and targeting moiety is stable in blood circulation, and it is easy to be broken in acidic microenvironment. These characteristics can be used to control the release of drug.^{34,35}

It is well-documented that the BPs preferentially deposit in metastatic bone lesions after systemic administration of BPs. HA is a major component of bone. The binding mechanism of BPs with HA is simple adsorption.¹⁸ In this paper, the HA adsorption experiment was performed to evaluate the adsorption capacity of ALN-MA-hyd-DOX with bone. The results indicated that the adsorption capacity of the ALN-MA-ami-DOX and ALN-MA-hyd-DOX with HA was significantly higher than that of DOX. No significant difference was observed in adsorption capacity between ALN-MA-ami-DOX and ALN-MA-hyd-DOX.

The ideal bone-targeted conjugates should not only have high binding affinity with bone but can also release drug at the desired site. The drug release characteristics from natural bone (immobilized ALN-MA-hyd-DOX and ALN-MA-ami-DOX) in different pH medium were investigated. The results showed that immobilized ALN-MA-hyd-DOX released DOX in pH-dependent manner. The higher DOX release rate of ALN-MA-hyd-DOX was observed at pH 5.0 and pH 6.0. This implied that ALN-MA-hyd-DOX was able to release large amount of DOX in sites of bone metastasis,⁶ thereby greatly enhancing the efficacy of DOX. There was a little amount of DOX released from immobilized ALN-MA-hyd-DOX in pH 7.4 medium. This indicated that ALN-MA-hyd-DOX was stable in blood circulation. On the contrary, a little amount of DOX was released from immobilized ALN-MA-ami-DOX in different pH medium. This implied that ALN-MA-ami-DOX could not exert obvious antitumor activity in sites of bone metastasis.

Alendronate-monoethyl adipate-(hydrazone)-doxorubicin conjugate showed much higher cytotoxicity on A549 cells and MDA-MB-231/ADR cells than that of ALN-MA-ami-DOX. ALN-MA-hyd-DOX showed the same cytotoxicity as free DOX did on A549 cells in 24 h. However, ALN-MA-hyd-DOX exhibited much higher cytotoxicity on A549 cells than free DOX did in 48 h. This was because when ALN-MA-hyd-DOX was uptaken by the tumor cell, the hydrazone bond was broken, which resulted in the release of DOX and ALN-MA in the tumor cell. It is reported that ALN inhibits farnesyl diphosphate synthase, and subsequently inhibits protein prenylation of tumor cells, which leads to apoptosis of the cell.³⁶ Zoledronate, a new generation of BPs, can work synergistically with

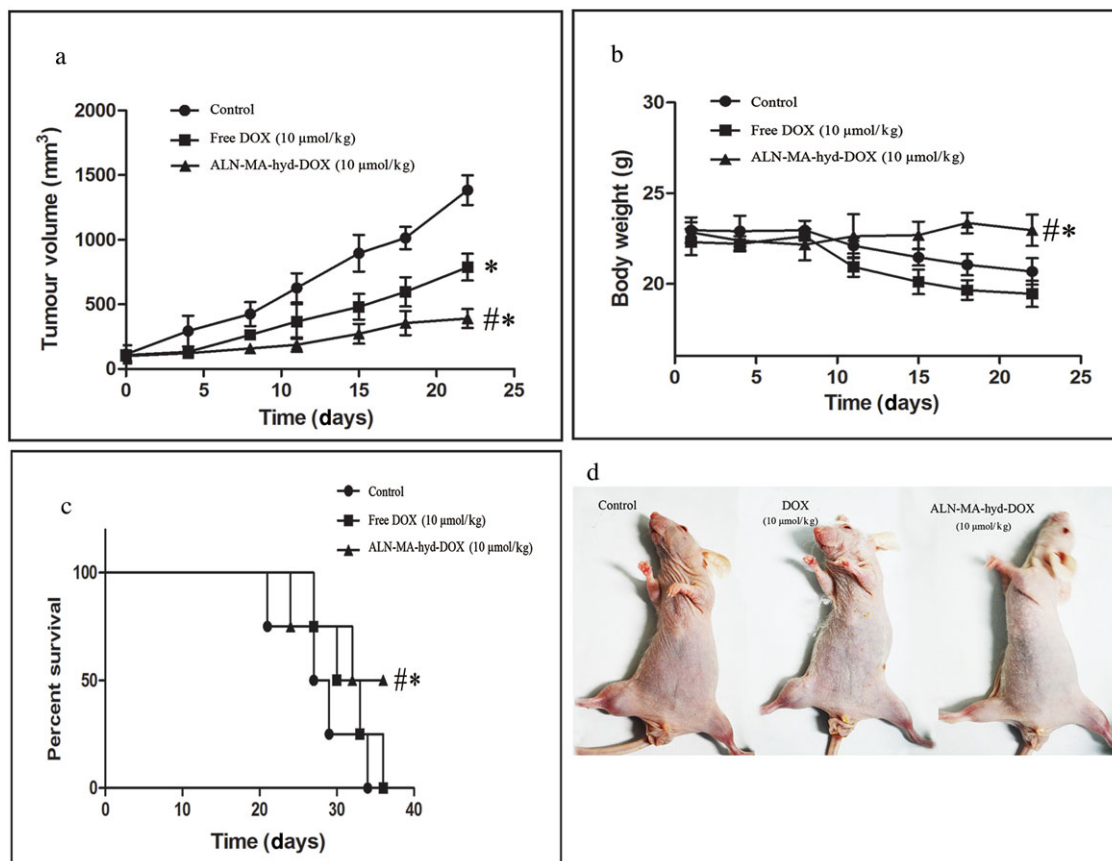


Figure 11. The *in vivo* antitumor activity of ALN-MA-hyd-DOX on tumor-bearing nude mice. (a) Tumor volume changes in tumor-bearing nude mice. (b) Body weight changes in tumor-bearing nude mice. (c) Survival curve of tumor-bearing mice. (d) Tumor-bearing nude mice recorded by camera at the end of the treatment. Female athymic nude mice were injected via intratibia with A549 cells. Treatment was initiated on the 10th day after tumor cell inoculation. Data are presented as the mean \pm standard deviation. * $p < 0.05$ versus control group at the end of the experiment ($n = 3$). # $p < 0.05$ versus DOX-treated group at the end of the experiment ($n = 3$).

DOX and decrease tumor growth *in vivo* in multiple tumor types.^{37,38}

The cellular uptake was observed by fluorescence microscopy. After A549 cells were treated with free DOX, the fluorescence mainly localized in nucleus. When A549 cells were treated with ALN-MA-ami-DOX, fluorescence was mainly localized in the cytoplasm, which resulted in the lower antitumor activity of ALN-MA-ami-DOX on A549 cells. However, when A549 cells were treated with ALN-MA-hyd-DOX, the fluorescence localized both in cytoplasm and nucleus. Previous studies demonstrated that cellular uptake of BP drugs required fluid-phase endocytosis, and BP usually localized in endolysosome.³⁹ Thus, the hydrazone bond of ALN-MA-hyd-DOX was broken in endolysosome, and DOX was released and diffused to cytoplasm and nucleus to exhibit its antitumor activity. When MDA-MB-231/ADR cells were treated with free DOX, little amount of the fluorescence was found in the nucleus and cytoplasm. Compared with the free DOX, when MDA-MB-231/ADR cells were incubated with ALN-MA-hyd-DOX and ALN-MA-ami-DOX, a large amount of the fluorescence was found in the nucleus and cytoplasm, which resulted in the higher cytotoxicity of ALN-MA-hyd-DOX and ALN-MA-ami-DOX than that of free DOX on MDA-MB-231/ADR cells. P-glycoprotein is an important protein of the cell membrane that pumps many foreign substances out of tumor cells and leads to drug resistance.⁴⁰ Although

DOX is a substrate of P-glycoprotein, the structure of ALN-MA-hyd-DOX and ALN-MA-ami-DOX is different from DOX. So, either ALN-MA-hyd-DOX or ALN-MA-ami-DOX is probably not a suitable substrate of P-glycoprotein. Furthermore, it was reported that ALN-modified drug delivery system had a potential of inhibiting P-glycoprotein by affecting ATPase activity and MDR1 gene expression.⁴¹ Thus, ALN-MA-hyd-DOX and ALN-MA-ami-DOX probably bypass P-glycoprotein-mediated drug efflux, and efficiently accumulate in drug-resistant cells. The exact mechanism that the cellular uptake of ALN-MA-hyd-DOX increased compared with free DOX in drug-resistant cell needs further investigation.

Although neither DOX nor ALN-MA-hyd-DOX could completely stop the growth of tumor, the tumor growth in drug-treated groups was obviously delayed. Compared with DOX, ALN-MA-hyd-DOX exhibited stronger antitumor activity, longer life span, and less toxicity on heart and kidney. This was because after ALN-MA-hyd-DOX was intravenously administered to tumor-bearing mice, DOX was mainly distributed in leg bone tumor tissue; a little amount of DOX was distributed in heart and kidney. However, after free DOX was administered to tumor-bearing mice, besides distributed in leg bone tumor tissue, some amount of DOX was distributed in heart and kidney, which resulted in significant damage in heart and kidney.

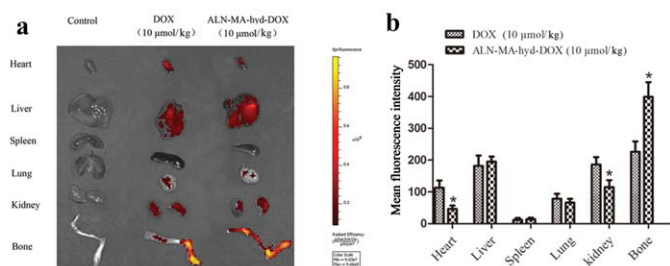


Figure 12. (a) Tissue distribution of DOX detected by *in vivo* image at 24 h after free DOX (10 μmol/kg) and ALN-MA-hyd-DOX (10 μmol/kg) was injected to tumor-bearing mice via the tail vein. (b) Semiquantitative analysis for the biodistribution of DOX at 24 h after free DOX (10 μmol/kg) and ALN-MA-hyd-DOX (10 μmol/kg) was injected to tumor-bearing mice via the tail vein. Data are presented as the mean ± standard deviation. * $p < 0.05$ versus DOX-treated group ($n = 3$).

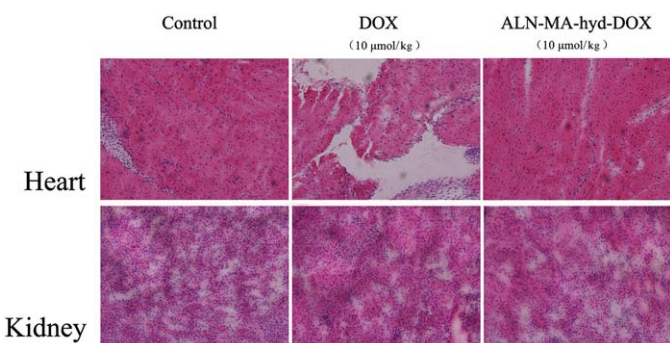


Figure 13. The representative H&E staining sections of heart and kidney from tumor-bearing nude mice with different treatments.

CONCLUSION

Alendronate-monoethyl adipate-(hydrazine)-doxorubicin conjugate showed high adsorption capacity with HA and natural bone. Natural bone immobilized ALN-MA-hyd-DOX released DOX in a pH-dependent manner. ALN-MA-hyd-DOX induced more apoptosis and showed high cytotoxicity on wild-type tumor cells and DOX-resistant tumor cells. Compared with the same dose of free DOX, ALN-MA-hyd-DOX significantly delayed tumor growth in tumor-bearing nude mice without obviously systemic toxicity. These findings implied that ALN-MA-hyd-DOX was a promising bone-targeted conjugate for treating bone neoplasms.

ACKNOWLEDGMENT

This research was supported by the Shaanxi Science and Technology Innovation Project (2012KTCL03-18).

REFERENCES

- Diel IJ, Solomayer EF, Bastert G. 2000. Treatment of metastatic bone disease in breast cancer: Bisphosphonates. *Clin Breast Cancer* 1(1):43–51.
- Mundy GR. 2002. Metastasis to bone: Causes, consequences and therapeutic opportunities. *Nat Rev Cancer* 2(8):584–593.
- Walker MS, Miller PJ, Namjoshi M, Houts AC, Stepanski EJ, Schwartzberg LS. 2013. Relationship between incidence of fracture and

health-related quality-of-life in metastatic breast cancer patients with bone metastases. *J Med Econ* 16(1):179–189.

4. Kingsley LA, Fournier PG, Chirgwin JM, Guise TA. 2007. Molecular biology of bone metastasis. *Mol Cancer Ther* 6(10):2609–2617.

5. Baron R, Neff L, Louvard D, Courtoy PJ. 1985. Cell-mediated extracellular acidification and bone resorption: Evidence for a low pH in resorbing lacunae and localization of a 100-kD lysosomal membrane protein at the osteoclast ruffled border. *J Cell Biol* 101(6):2210–2222.

6. Teitelbaum SL. 2000. Bone resorption by osteoclasts. *Science* 289(5484):1504–1508.

7. Bae Y, Nishiyama N, Fukushima S, Koyama H, Yasuhiro M, Kataoka K. 2005. Preparation and biological characterization of polymeric micelle drug carriers with intracellular pH-triggered drug release property: Tumor permeability, controlled subcellular drug distribution, and enhanced *in vivo* antitumor efficacy. *Bioconj Chem* 16(1):122–130.

8. Oh KT, Kim D, You HH, Ahn YS, Lee ES. 2009. pH-sensitive properties of surface charge-switched multifunctional polymeric micelle. *Int J Pharm* 376(1–2):134–140.

9. Ye WL, Teng ZH, Liu DZ, Cui H, Liu M, Cheng Y, Yang TH, Mei QB, Zhou SY. 2013. Synthesis of a new pH-sensitive folate-doxorubicin conjugate and its antitumor activity *in vitro*. *J Pharm Sci* 102(2):530–540.

10. Liang CH, Ye WL, Zhu CL, Na R, Cheng Y, Cui H, Liu DZ, Yang ZF, Zhou SY. 2014. Synthesis of doxorubicin alpha-linolenic acid conjugate and evaluation of its antitumor activity. *Mol Pharm* 11(5):1378–1390.

11. Fazil M, Baboota S, Sahni JK, Ameeruzzafar, Ali J. 2015. Bisphosphonates: Therapeutics potential and recent advances in drug delivery. *Drug Deliv* 22(1):1–9.

12. Ferretti G, Fabi A, Carlini P, Papaldo P, Felici A, Tomao S, Cognetti F. 2007. Zoledronic acid and angiogenesis. *Clin Cancer Res* 13(22 Pt 1):6850–6851.

13. Seymour LW, Ferry DR, Anderson D, Hesslewood S, Julyan PJ, Poyner R, Doran J, Young AM, Burtles S, Kerr DJ. 2002. Hepatic drug targeting: Phase I evaluation of polymer-bound doxorubicin. *J Clin Oncol* 20(6):1668–1676.

14. Gittens SA, Bansal G, Zernicke RF, Uludag H. 2005. Designing proteins for bone targeting. *Adv Drug Deliv Rev* 57(7):1011–1036.

15. Uludag H, Yang J. 2002. Targeting systemically administered proteins to bone by bisphosphonate conjugation. *Biotechnol Prog* 18(3):604–611.

16. El-Mabhouth AA, Angelov CA, Cavell R, Mercer JR. 2006. A 99mTc-labeled gemcitabine bisphosphonate drug conjugate as a probe to assess the potential for targeted chemotherapy of metastatic bone cancer. *Nucl Med Biol* 33(6):715–722.

17. Bagi CM. 2005. Targeting of therapeutic agents to bone to treat metastatic cancer. *Adv Drug Deliv Rev* 57(7):995–1010.

18. Sevcik MA, Luger NM, Mach DB, Sabino MA, Peters CM, Ghilardi JR, Schwei MJ, Rohrich H, De Felipe C, Kuskowski MA, Mantyh PW. 2004. Bone cancer pain: The effects of the bisphosphonate alendronate on pain, skeletal remodeling, tumor growth and tumor necrosis. *Pain* 111(1–2):169–180.

19. Tuomela JM, Valta MP, Vaananen K, Harkonen PL. 2008. Alendronate decreases orthotopic PC-3 prostate tumor growth and metastasis to prostate-draining lymph nodes in nude mice. *BMC Cancer* 8:81.

20. Molinuevo MS, Bruzzone L, Cortizo AM. 2007. Alendronate induces anti-migratory effects and inhibition of neutral phosphatases in UMR106 osteosarcoma cells. *Eur J Pharmacol* 562(1–2):28–33.

21. Hashimoto K, Morishige K, Sawada K, Tahara M, Kawagishi R, Ikebuchi Y, Sakata M, Tasaka K, Murata Y. 2005. Alendronate inhibits intraperitoneal dissemination in *in vivo* ovarian cancer model. *Cancer Res* 65(2):540–545.

22. Choi SW, Kim JH. 2007. Design of surface-modified poly (D,L-lactide-co-glycolide) nanoparticles for targeted drug delivery to bone. *J Control Release* 122(1):24–30.

23. Wright JE, Gittens SA, Bansal G, Kitov PI, Sindrey D, Kucharski C, Uludag H. 2006. A comparison of mineral affinity of bisphosphonate-protein conjugates constructed with disulfide and thioether linkages. *Biomaterials* 27(5):769–784.

24. Doschak MR, Kucharski CM, Wright JE, Zernicke RF, Uludag H. 2009. Improved bone delivery of osteoprotegerin by bisphosphonate conjugation in a rat model of osteoarthritis. *Mol Pharm* 6(2):634–640.
25. Long JT, Cheang TY, Zhuo SY, Zeng RF, Dai QS, Li HP, Fang S. 2014. Anticancer drug-loaded multifunctional nanoparticles to enhance the chemotherapeutic efficacy in lung cancer metastasis. *J Nanobiotechnol* 30(1):37.
26. Su D, Cheng Y, Liu M, Liu D, Cui H, Zhang B, Zhou S, Yang T, Mei Q. 2013. Comparison of piceid and resveratrol in antioxidation and antiproliferation activities in vitro. *PLoS One* 8(1):e54505.
27. Balas F, Manzano M, Horcajada P, Vallet-Regi M. 2006. Confinement and controlled release of bisphosphonates on ordered mesoporous silica-based materials. *J Am Chem Soc* 128(25):8116–8117.
28. Colleoni M, O'Neill A, Goldhirsch A, Gelber RD, Bonetti M, Thurlimann B, Price KN, Castiglione-Gertsch M, Coates AS, Lindtner J, Collins J, Senn HJ, Cavalli F, Forbes J, Gudgeon A, Simoncini E, Cortes-Funes H, Veronesi A, Fey M, Rudenstam CM. 2000. Identifying breast cancer patients at high risk for bone metastases. *J Clin Oncol* 18(23):3925–3935.
29. Janjan N, Lutz ST, Bedwinek JM, Hartsell WF, Ng A, Pieters RJ, Ratanatharathorn V, Silberstein EB, Taub RJ, Yasko AW, Rettenmaier A. 2009. Therapeutic guidelines for the treatment of bone metastasis: A report from the American College of Radiology Appropriateness Criteria Expert Panel on Radiation Oncology. *J Palliat Med* 12(5):417–426.
30. Gonzalez-Angulo AM, Morales-Vasquez F, Hortobagyi GN. 2007. Overview of resistance to systemic therapy in patients with breast cancer. *Adv Exp Med Biol* 608:1–22.
31. Kozlow W, Guise TA. 2005. Breast cancer metastasis to bone: Mechanisms of osteolysis and implications for therapy. *J Mammary Gland Biol Neoplasia* 10(2):169–180.
32. Yoneda T, Hiraga T. 2005. Crosstalk between cancer cells and bone microenvironment in bone metastasis. *Biochem Biophys Res Commun* 328(3):679–687.
33. Arnett T. 2003. Regulation of bone cell function by acid-base balance. *Proc Nutr Soc* 62(2):511–520.
34. Ulbrich K, Subr V. 2004. Polymeric anticancer drugs with pH-controlled activation. *Adv Drug Deliv Rev* 56(7):1023–1050.
35. Chytil P, Etrych T, Konak C, Sirova M, Mrkvan T, Rihova B, Ulbrich K. 2006. Properties of HPMA copolymer-doxorubicin conjugates with pH-controlled activation: Effect of polymer chain modification. *J Control Release* 115(1):26–36.
36. Roelofs AJ, Thompson K, Gordon S, Rogers MJ. 2006. Molecular mechanisms of action of bisphosphonates: Current status. *Clin Cancer Res* 12(20 Pt 2):6222s–6230s.
37. Clyburn RD, Reid P, Evans CA, Lefley DV, Holen I. 2010. Increased anti-tumour effects of doxorubicin and zoledronic acid in prostate cancer cells in vitro: Supporting the benefits of combination therapy. *Cancer Chemother Pharmacol* 65(5):969–978.
38. Ottewell PD, Deux B, Monkkonen H, Cross S, Coleman RE, Clezardin P, Holen I. 2008. Differential effect of doxorubicin and zoledronic acid on intraosseous versus extraosseous breast tumor growth in vivo. *Clin Cancer Res* 14(14):4658–4666.
39. Thompson K, Rogers MJ, Coxon FP, Crockett JC. 2006. Cytosolic entry of bisphosphonate drugs requires acidification of vesicles after fluid-phase endocytosis. *Mol Pharmacol* 69(5):1624–1632.
40. Ling V. 1997. Multidrug resistance: Molecular mechanisms and clinical relevance. *Cancer Chemother Pharmacol* 40(8):S3–S8.
41. Negi LM, Talegaonkar S, Jaggi M, Verma AK, Verma R, Dobhal S, Kumar V. 2014. Surface engineered nanostructured lipid carriers for targeting MDR tumor: Part I. Synthesis, characterization and in vitro investigation. *Colloids Surf B Biointerfaces* 123(8):600–609.